

Supplementary Information

Droplet size affects the degree of separation between fluorescence-positive and fluorescence-negative droplet populations in droplet digital PCR

Yusuke Nakamura^a and Masahiko Hashimoto^{*,a}

^aDepartment of Chemical Engineering and Materials Science, Faculty of Science and Engineering, Doshisha University, 1-3 Tataramiyakodani, Kyotanabe, Kyoto 610-0321, Japan

***Correspondence:** Prof. Masahiko Hashimoto, Department of Chemical Engineering and Materials Science, Faculty of Science and Engineering, Doshisha University, 1-3 Tataramiyakodani, Kyotanabe, Kyoto 610-0321, Japan

E-mail: mahashim@mail.doshisha.ac.jp

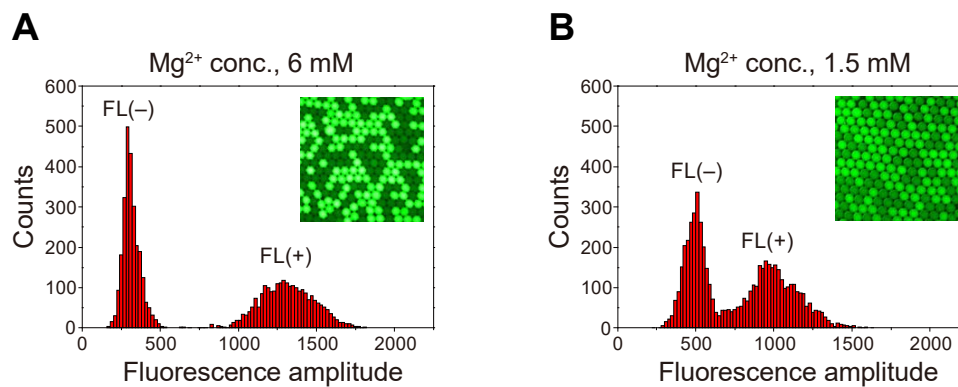
Fax: +81-774-65-6594

Table of Contents

- 1 Figure S1 Histograms of the fluorescence amplitude for ddPCR readouts**

- 2 ddPCR experiments**
 - 2.1 Microfluidic droplet preparation setup**
 - 2.2 Figure S2 Schematic drawings of the microchannel patterns**
 - 2.3 Figure S3 Microfluidic droplet production system based on a PZT micropump**
 - 2.4 Operational steps**
 - 2.5 Table S1 Oligonucleotide sequences used for PCR**

1 Figure S1 Histograms of the fluorescence amplitude for ddPCR readouts



Influence of Mg^{2+} concentration in a PCR cocktail on the separation of populations of fluorescence-positive (FL(+)) and fluorescence-negative (FL(-)) droplets. The Mg^{2+} concentration in the PCR cocktail was: (A) 6 mM and (B) 1.5 mM. The clusters of FL(+) are FL(-) droplets are clearly separated in (A) but not in (B). These histograms were adapted from our previous publication in a RSC journal [1] with slight modifications.

2 ddPCR experiments

2.1 Microfluidic droplet preparation setup

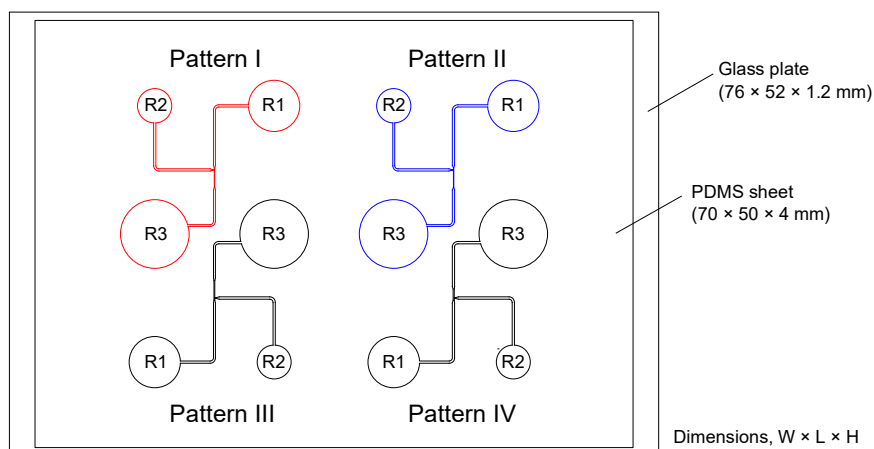
Custom polydimethylsiloxane (PDMS) microfluidic sheets (70 mm × 50 mm × 4 mm), fabricated by standard soft lithography, were obtained from YODAKA (Kanagawa, Japan) (Figure S2). The structure of the sheets consisted of four T-junction patterns of microchannels with a common channel length but different depths and widths. The channel depths were 50 μm (Pattern I), 75 μm (Pattern II), or 100 μm (Patterns III and IV), and the width was identical to the depth in each pattern at the T-junction (i.e., cross-sectional channel dimensions of 50 μm × 50 μm (Pattern I), 75 μm × 75 μm (Pattern II), and 100 μm × 100 μm (Patterns III and IV), respectively). The T-junction consisted of a continuous-phase (oil) channel and a dispersed-phase (aqueous solution) channel connected perpendicularly. The channel widths in the microfluidic chip increased from the aforementioned dimensions at the T-junction to 250 μm at up- and downstream points on the flow path. The only structural difference between Patterns III and IV was the downstream length of the narrowed channel at the T-junction (specifically, 2 mm for Pattern III and 1 mm for Pattern IV). The channels terminated at their respective reservoirs (R1, R2, and R3 in Figure S2). The capacities of R1, R2, and R3 were 113, 50, and 201 μL, respectively. The PDMS sheet was reversibly adhered to a 76 mm × 52 mm × 1.2 mm glass slide through the viscoelasticity of PDMS.

A commercially available piezoelectric (PZT) diaphragm micropump (SDMP306; Takasago Electric, Nagoya, Japan) with a model-specific controller (MPC-200A; Takasago Electric) was used to acquire fluid flows in the microchannels (Figure S3A). The controller generated a standard wave (modified sine wave) voltage to actuate the PZT pump element.

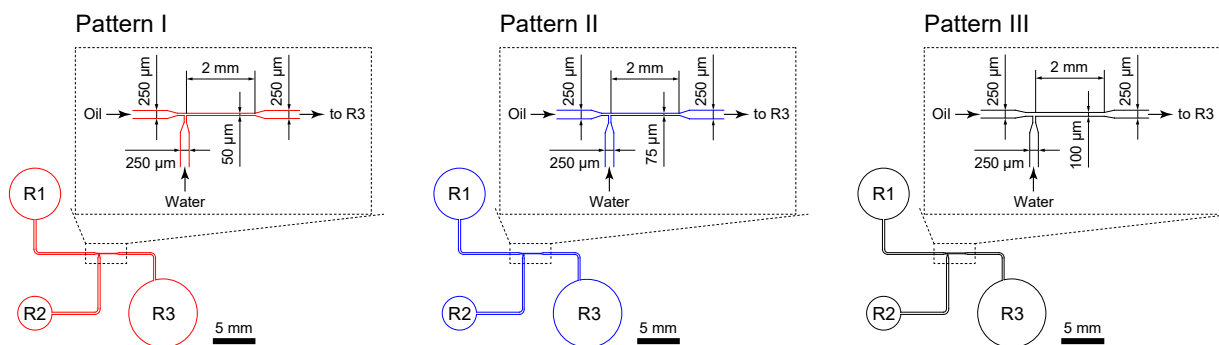
A custom square rod of aluminum, with a threaded screw hole containing a coaxial through-hole of a smaller diameter, was placed on the PDMS microfluidic chip such that the through-hole was located immediately above the outlet reservoir (R3). The PDMS/glass microchip and aluminum rod setup were then clamped together in a custom aluminum holder. The PDMS/aluminum boundary was sufficiently gas-tight owing to the viscoelasticity of PDMS. One end of a short PTFE tube was connected to the through-hole within the aluminum rod by fitting a gas-tight nut into the threaded screw hole (see Figure S3B, showing an enlarged cross-sectional view of the architecture at R3). A short Tygon tube was employed to connect the other end of the PTFE tube to an inlet pipe protruding from the PZT pump. This pump configuration could remove air within R3 to create a reduced pressure environment inside.

2.2 Figure S2 Schematic drawings of the microchannel patterns

A

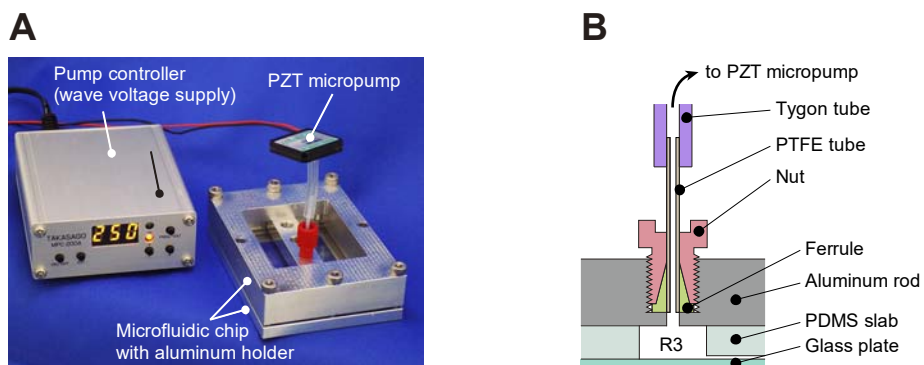


B



(A) Configuration of four T-junction patterns of microchannels (Patterns I, II, III, and IV) with terminal reservoirs (R1 for oil loading, R2 for aqueous-phase loading, and R3 for droplet collection) on a PDMS sheet. The depths of the channels drawn with red, blue, and black lines were 50, 75, and 100 μm , respectively. (B) Individual drawings with enlarged views of the T-channel junctions for Patterns I–III. The geometry of Pattern IV only differed from that of Pattern III in the length of the narrowed channel downstream of the T-channel junction (1 mm for Pattern I and 2 mm for Pattern III). A drawing for Pattern IV is omitted in (B) because it was not used in the present study.

2.3 Figure S3 Microfluidic droplet production system based on a PZT micropump



(A) Photograph of the setup, comprising the microfluidic assembly, piezoelectric (PZT) diaphragm micropump, and pump controller. (B) An enlarged cross-sectional view of the architecture at R3. The photograph and the illustration were adapted with slight modifications from our previous publication [2] with permission from John Wiley and Sons.

2.4 Operational steps

Lambda DNA (New England Biolabs Japan K.K., Tokyo, Japan) was used as template DNA for PCR amplification by adding a defined copy number to 20 μL of solution containing 1 \times ddPCR Supermix for Probes (Bio-Rad, Hercules, CA, USA), 0.5 μM forward and reverse primers, which amplify 76 bp product, and 0.2 μM probe. See Table S1 for the sequences of the primer set and the probe labeled with HEX and BHQ-2 at the 5' and 3' ends, respectively.

The operational procedures involved in the ddPCR experiments are schematically shown in Figure 1 in the main text. Oil (70 μL ; Droplet Generation Oil for Probes, Bio-Rad) was dispensed into inlet reservoir R1 and 20 μL of the aforementioned aqueous reaction mixture for PCR amplification was added to inlet reservoir R2. Then, the microfluidic chip was set in the PZT diaphragm micropump-based fluid manipulation system depicted in Figure S3 to achieve fluid flows in the microchannels. The full details of the fluid control system are provided in our previous publications [2,3]. A peak-to-peak drive voltage of 250 V_{p-p} at a frequency of 60 Hz was applied to the micropump to remove air from the sealed outlet reservoir (R3). The pressure difference created between the outlet and inlet reservoirs drew the preloaded oil and aqueous solution into the channels, generating water-in-oil droplets at the downstream T-channel junction (Figure 1A in the main text). We used three of the four T-junctions of the microchannels shown in Figure S2 (Patterns I, II, and III), which generated droplets approximately 62, 92, and 126 μm in diameter, respectively.

After terminating droplet formation, droplets accumulated in the outlet reservoir (R3) were gently collected using a micropipette and dispensed into a conventional PCR tube for subsequent PCR amplification (Main Text Figure 1B). Using a commercial thermal cycler (Thermo Fisher Scientific K.K., Tokyo, Japan), the droplets in the tube were initially heated for 10 min at 95 $^{\circ}\text{C}$, and then thermally cycled 40 times for 30 s at 94 $^{\circ}\text{C}$ and 60 s at 63 $^{\circ}\text{C}$, followed by a final holding of 10 min at 98 $^{\circ}\text{C}$. The reaction was terminated by rapid cooling to 4 $^{\circ}\text{C}$ in the thermal cycler.

After thermal cycling, the droplets were carefully collected using a micropipette, and slowly injected into a shallow chamber fabricated from PDMS, forming a droplet monolayer inside. Fluorescence images of the droplet monolayers were acquired using an inverted fluorescence microscope equipped with an electron multiplier charge-coupled device (EMCCD) camera (Main Text Figure 1C). Fluorescence intensities of droplets present in the images were measured using software bundled with the EMCCD camera (Main Text Figure 1D).

2.5 Table S1 Oligonucleotide sequences used for PCR

oligos	usage	sequences (5'→3')	size (mer)
Forward	PCR amplification	CCCAGCAACAGCACAAACCC	19
Reverse	PCR amplification	GCCGCAGCGTAACTATTACTAATG	24
Probe	Fluorescence signaling	^a HEX-ACTGAGCCGTAGCCACTGTCTGTCCT-BHQ-2 ^b	26

^aHEX, $\lambda_{\text{ex}} = 538 \text{ nm}$, $\lambda_{\text{em}} = 555 \text{ nm}$. ^bBHQ-2, Black Hole Quencher-2 as a quencher molecule ($\lambda_{\text{abs, max}} = 578 \text{ nm}$).

References

- [1] Takahara, H., Matsushita, H., Inui, E., Ochiai, M., Hashimoto, M., *Anal. Methods* 2021, 13, 974–985.
- [2] Oda, Y., Oshima, H., Nakatani, M., Hashimoto, M., *Electrophoresis* 2019, 40, 414–418.
- [3] Okura, N., Nakashoji, Y., Koshirogane, T., Kondo, M., Tanaka, Y., Inoue, K., Hashimoto, M., *Electrophoresis* 2017, 38, 2666–2672.